

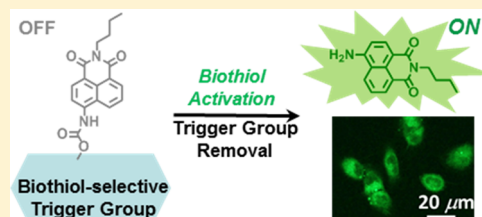
# Rapid, Photoinduced Electron Transfer-Modulated, Turn-on Fluorescent Probe for Detection and Cellular Imaging of Biologically Significant Thiols

Rasika R. Nawimanage, Bijeta Prasai, Suraj U. Hettiarachchi, and Robin L. McCarley\*

Department of Chemistry, Louisiana State University, Baton Rouge, Louisiana 70803-1804, United States

## S Supporting Information

**ABSTRACT:** There is a very limited number of existing probes whose fluorescence is turned on in the presence of the class of biological thiols made up of glutathione, cysteine, and homocysteine. The extant probes for this class of biological thiols commonly have poor aqueous solubility and long analyte response times, and they demand a very high probe/thiol ratio for decreased time of significant reporter signal generation; knowledge regarding their selectivity with respect to other sulfur-based analytes is unclear. Described here is a previously unreported photoinduced electron-transfer-quenched probe (HMBQ-Nap 1) that offers highly selective and rapid in vitro detection of this class of biologically important thiols at low concentrations and low probe/thiol ratio, and importantly, very rapid imaging of these biological thiols in human cells.



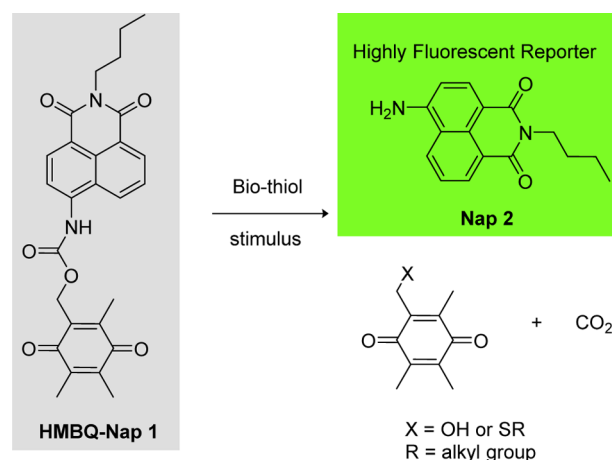
The need is great for a diverse set of probes capable of having their fluorescence signal turned on by analytes in complex environments, so as to allow for analyte detection, quantification, and imaging.<sup>1</sup> Diversity is required for both the mechanism of analyte activation of the probe to reveal its corresponding highly fluorescent reporter, and the energy range over which the reporter provides a signal of analyte presence. Ideally, beyond probes whose signal is so selective that determination of a single target is deemed specific, the library will possess probes that offer class-selective detection and quantification of analytes with high figures of merit. The latter is of great value in complicated analysis scenarios, which often also require rapid and temporally stable reporting of analyte presence.

Currently, there is a small group of environmentally stable probes whose fluorescence is turned on in the complex medium of mammalian cells only by the collective presence of the biologically relevant thiol compounds<sup>2</sup> glutathione (GSH), cysteine (Cys), and homocysteine (Hcy).<sup>3</sup> These efforts to detect and image intracellularly the presence of this class of biological thiols have employed turn-on probes that, for the most part, are poorly soluble in physiologically relevant media, have long analyte response times, and/or require excessive amounts of analyte to achieve timely activation of the probe to yield a measurable reporter signal. Furthermore, the GSH/Cys/Hcy selectivity of these previously reported probes with regard to presence of H<sub>2</sub>S or protein thiols is not known, quite poor, or limited<sup>4</sup> at best. Thus, due to the crucial role that GSH, Cys, and Hcy play in biological systems, particularly within cells, it is important to develop probes that are passively taken up by cells in a quick fashion; whose fluorescence signal is rapidly turned on in the presence of these three biological thiols while remaining fluorescently silent upon exposure to other bio-

logically important analytes, and whose fluorescence background response in comparison to the signal of the reporter is exceedingly small (minimal spectral overlap of probe and reporter absorption/emission) so as to allow for cellular imaging with high contrast (large signal-to-background ratio).

To that end, we report herein the design, synthesis, and evaluation of the turn-on probe HMBQ-Nap 1 (Scheme 1). This new probe offers exceedingly rapid (<5 min) and low-concentration (~30 nM) detection of GSH, Cys, and Hcy under physiological conditions, without the need for excessively

## Scheme 1. Biological Thiol Activation of HMBQ-Nap 1

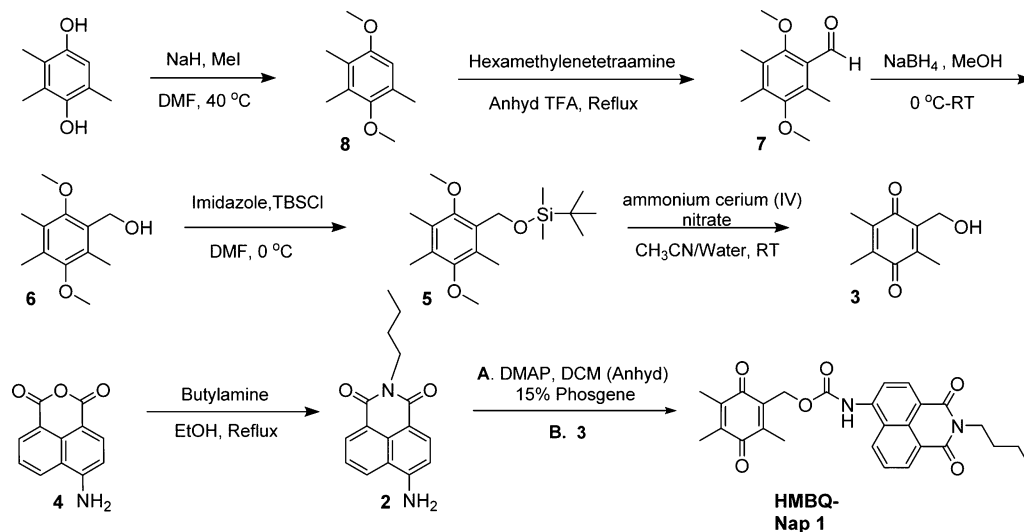


Received: September 12, 2014

Accepted: October 24, 2014

Published: October 24, 2014

Scheme 2. Synthetic Route for HMBQ-Nap 1 Probe



high probe/analyte ratios to achieve rapid probe activation or the requirement for large amounts of organic cosolvent to boost probe solubility. HMBQ-Nap 1 exhibits remarkably good selectivity toward these thiols in comparison to a protein thiol and the gasotransmitter  $\text{H}_2\text{S}$  that is of growing interest to the cell measurement science community. Importantly, due to its design, HMBQ-Nap 1 is taken up and activated in a very rapid fashion, so as to offer high-speed imaging of total intracellular biological thiol content in human cells with a high signal-to-background ratio.

## EXPERIMENTAL SECTION

**Materials and General Methods.** Column purifications were performed by use of SNAP silica columns on a Flashmaster Personal from Biotage. All chemicals were purchased from Sigma–Aldrich or Fisher Scientific. Thin-layer chromatography was performed on aluminum-backed 60 F254 silica plates from EMD Chemicals Inc. The  $^1\text{H}$  NMR and  $^{13}\text{C}$  NMR spectra were collected in  $\text{CDCl}_3$  or deuterated dimethyl sulfoxide ( $\text{DMSO}-d_6$ ) at  $25^\circ\text{C}$  on a Bruker AV-400 spectrometer, with chemical shifts reported in the standard  $\delta$  notation of parts per million, with tetramethylsilane as an internal reference. Absorption bands in NMR spectra are listed as singlet (s), doublet (d), triplet (t), or multiplet (m), and the coupling constants  $J$  are expressed in hertz (Hz). Mass spectral analyses were carried out on an Agilent 6210 electrospray ionization time-of-flight mass spectrometer (ESI-TOFMS). All solutions were prepared with Nanopure water from a Barnstead Diamond Nanopure water System ( $18\text{ M}\Omega\cdot\text{cm}$ ).

**Synthesis.** Synthesis of HMBQ-Nap 1 is as outlined in Scheme 2. The free Nap 2 reporter, 4-amino-9-(*n*-butyl)-1,8-naphthalimide, and compound 3, hydroxymethylbenzoquinone (HMBQ),<sup>5</sup> were synthesized according to literature methods.

To a solution of 2 (36.39 mg, 0.14 mmol) in anhydrous dichloromethane (DCM) were added 4-dimethylaminopyridine (DMAP; 32.92 mg, 0.27 mmol) and a solution of phosgene (15% toluene, 1 mL) at  $-10^\circ\text{C}$ , and the mixture was stirred under argon for 3 h. The excess phosgene was removed by bubbling argon gas through the solution for 30 min. To this resulting solution was added 3 (70.39 mg, 0.39 mmol), and the solution was stirred at  $0^\circ\text{C}$  for an additional 12 h. The reaction mixture was quenched with water (30 mL) and extracted with

$\text{CH}_2\text{Cl}_2$  ( $3 \times 50\text{ mL}$ ). The organic phase was dried over  $\text{Na}_2\text{SO}_4$ , subsequently filtered, and the solvent was evaporated. The crude product was purified by silica gel flash column chromatography using dichloromethane/ethyl acetate (10:1 v/v). The final product was obtained as a yellow solid.  $^1\text{H}$  NMR (400 MHz,  $\text{DMSO}-d_6$ )  $\delta$  10.30 (s, 1H), 8.65 (dd,  $J = 8.8, 3.7\text{ Hz}$ , 1H), 8.57–8.43 (m, 2H), 8.16 (dd,  $J = 8.3, 3.7\text{ Hz}$ , 1H), 7.82 (td,  $J = 8.2, 3.6\text{ Hz}$ , 1H), 5.14 (d,  $J = 3.5\text{ Hz}$ , 2H), 4.03 (q,  $J = 6.0, 4.4\text{ Hz}$ , 2H), 2.15 (d,  $J = 3.7\text{ Hz}$ , 3H), 1.99 (d,  $J = 3.5\text{ Hz}$ , 6H), 1.61 (p,  $J = 7.4\text{ Hz}$ , 2H), 1.42–1.30 (m, 2H), 0.97–0.87 (m, 3H).  $^{13}\text{C}$  NMR (100 MHz,  $\text{DMSO}-d_6$ )  $\delta$  12.56, 12.72, 14.18, 20.26, 30.14, 58.52, 117.70, 118.89, 122.70, 124.40, 126.86, 128.78, 129.76, 131.37, 132.11, 136.80, 140.48, 141.14, 144.82, 154.19, 163.38, 163.92, 185.92, 187.42. ESI-MS for  $\text{C}_{27}\text{H}_{26}\text{N}_2\text{O}_6$ : expected  $m/z = 475.188$  [ $\text{M} + \text{H}$ ] $^+$ ; found  $m/z = 475.1864$  [ $\text{M} + \text{H}$ ] $^+$ ; 1.5 ppm error.

**Voltammetry.** Cyclic voltammetry was performed in 0.1 M (*n*-butyl) $_4\text{NClO}_4$ /dry acetonitrile under anaerobic conditions. A Princeton Applied Research model 273A potentiostat/galvanostat was used with the Power Suite 2.53 operating software. Voltammograms were collected at  $0.1\text{ V}\cdot\text{s}^{-1}$  at room temperature ( $25^\circ\text{C}$ ) after the solution was degassed with nitrogen for 20 min. Glassy-carbon working (BAS, 3 mm diameter), platinum wire counter, and Ag/AgCl reference (BAS) electrodes were used, and the potentials were referenced versus ferrocene/ferrocenium internal standard.

**Calculation of Free Energy of Photoinduced Electron Transfer.** To assess the thermodynamic feasibility of fluorescence quenching of HMBQ-Nap 1 by oxidative photoinduced electron transfer (OeT), voltammetric measurements of HMBQ-Nap 1 and its components were used in conjunction with the Rehm–Weller equation to calculate the free energy of the PeT process:

$$\Delta G_{\text{PeT}} = E_{\text{D}} - E_{\text{A}} - \Delta G_{00} - \frac{e^2}{\epsilon d} \quad (1)$$

For the OeT process, the redox potential ( $E_{\text{D}}$ ) of the donor Nap 2 and the potential ( $E_{\text{A}}$ ) of the acceptor HMBQ 3 were determined to be 1.24 and  $-0.92\text{ V}$ , respectively.  $\Delta G_{00}$ , the energy of the first excited singlet state of Nap 2, was found to be  $2.67\text{ eV}$ ;<sup>2</sup>  $e^2/\epsilon d$  is the Coulombic interaction energy of the ion pair, known to be  $0.06\text{ eV}$ . From these values, the energy

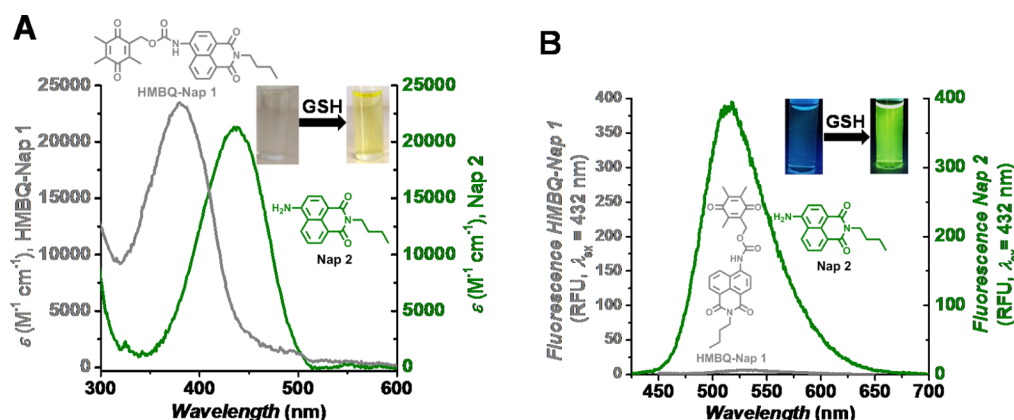


**Figure 1.** (A) Absorbance and (B) fluorescence spectra of 2  $\mu\text{M}$  HMBQ-Nap 1 (gray line) and 2  $\mu\text{M}$  Nap 2 (Green line) in 10% DMSO/90% 0.1 M phosphate-buffered saline (PBS), pH 7.4 at 25  $^{\circ}\text{C}$ . Insets: (A) visual color change and (B) fluorescence emission change observed for solution of HMBQ-Nap 1 upon addition of glutathione (GSH).

change for OeT quenching,  $\Delta G_{\text{PeT}}$  is calculated to be  $-0.95$  eV, indicating that electron transfer from the excited Nap 2 to the electron-poor HMBQ 3 is thermodynamically feasible.

**Spectroscopic Methods.** All spectroscopic measurements were performed in 0.1 M phosphate buffer/0.1 M KCl solutions, pH 7.4. Absorption spectra were recorded on a Varian Cary-50 spectrophotometer, and fluorescence data were collected on a PerkinElmer LS55 spectrometer. Samples for absorption and emission measurements were contained in 1 cm  $\times$  1 cm quartz cuvettes (3.5 mL volume, Sigma–Aldrich). Fluorescence quantum yields were determined by reference to coumarin in EtOH ( $\Phi = 0.54$ ) and quinine sulfate in 1 N  $\text{H}_2\text{SO}_4$  ( $\Phi = 0.51$ ).<sup>6</sup>

**Procedure for Thiol Sensing.** A stock solution of HMBQ-Nap 1 (100  $\mu\text{M}$ ) was prepared in 100% DMSO and was subsequently diluted to prepare appropriate concentration solutions of 1 in DMSO/phosphate-buffered saline (10% DMSO/90% 0.1 M PBS, pH 7.4). Thiol stock solutions were freshly prepared prior to each experiment. For the calibration curve, solutions of HMBQ-Nap 1 were incubated with different concentrations of thiols at 37  $^{\circ}\text{C}$  for 15 min, and spectral data were recorded. Excitation was at 432 nm and emission was detected at 540 nm. The excitation and emission slit widths were set at 2.5 nm.

**Cell Culture.** H596 (human non-small-cell lung cancer), cell culture base medium, and fetal bovine serum (FBS) were purchased from American Type Culture Collection (ATCC), Manassas, VA. Cell culture was performed as suggested by ATCC. H596 cells were cultured in RPMI-1640 with 10% FBS and 10 IU/mL penicillin–streptomycin. Cells were incubated at 37  $^{\circ}\text{C}$  in a humidified incubator containing 5 wt %/vol  $\text{CO}_2$ .

**Cell Imaging via Scanning Laser Confocal Microscopy.** H596 cells were cultured overnight in 22  $\times$  22 mm glass coverslips on a treated tissue culture 6-well plate purchased from Fisher Scientific. At that time, the existing growth medium was replaced with 2 mL of fresh medium and then incubated at 37  $^{\circ}\text{C}$ . Solutions of HMBQ-Nap 1 prepared in DMSO were added to the cells to give a  $2 \times 10^{-5}$  M solution of HMBQ-Nap 1, with the DMSO concentration kept constant at <1%. Cells were incubated with HMBQ-Nap 1 at 37  $^{\circ}\text{C}$  for 10 min and then treated with  $3.0 \times 10^{-6}$  M DRAQ5 (nuclear stain obtained from Thermo Scientific) for 1 min. The medium was removed and the cells were fixed in 2 mL of 4% paraformaldehyde for 15 min with shaking. After fixing, the cells were rinsed with

Nanopure water, and the coverslips were mounted to glass slides with Immumount (obtained from Fisher Scientific). Glass slides were left in the dark overnight to allow the Immumount to dry. Confocal images were acquired on a Leica TCS SP2 spectral confocal microscope. For images of cells exposed to HMBQ-Nap 1, samples were excited with the 458 nm line of an Ar/KrAr laser (laser intensity = 72%), and the spectral emission was collected (Leica DD458/514, 480–580 nm); photomultiplier tube (PMT) voltage = 710 V. Likewise, cells exposed to DRAQ5 were excited with the 633 nm line of a HeNe laser (laser intensity = 35%), and the spectral emission was collected (665–750 nm). All images were collected via a pinhole of 3.1 Airy units. Images were frame- and line-averaged four times. Image analysis was performed with ImageJ and Leica LAS AF lite software. As the control experiment, H596 cells were preincubated with 10 mM *N*-ethylmaleimide (NEM) at 37  $^{\circ}\text{C}$  for 30 min to scavenge all thiols in cells, then the cells were washed with 0.1 M, pH 7.4 PBS to remove any excess NEM, followed by incubation with 20  $\mu\text{M}$  HMBQ-Nap 1 prior to their being fixed as above.

## RESULTS AND DISCUSSION

**Design of Fluorescent Probe.** The design rationale of the PeT (photoinduced electron transfer) quenched fluorescence probe HMBQ-Nap 1 in Scheme 1 is as follows. HMBQ-Nap 1 contains 4-amino-9-(*n*-butyl)-1,8-naphthalimide (Nap 2) as the reporter unit and hydroxymethylbenzoquinone (HMBQ) as the oxidative PeT quencher, with the latter also being the pendant reaction site for biologically relevant thiols. The electronic properties of the HMBQ trigger group are such that HMBQ ( $E_{1/2} = -0.80$  V vs standard hydrogen electrode, SHE) should not be activated by possible interferents in biological milieu, for example, ascorbate and reduced nicotinamide adenine dinucleotide (NADH). In addition, the carbamate linkage between the HMBQ trigger group and the Nap 2 reporter was chosen due to its known stability in biological environments.<sup>7</sup> Thus, upon successful thiol–HMBQ-Nap 1 interaction (Michael addition that leads to elimination of thiol–HMBQ product and  $\text{CO}_2$ ), a highly intense fluorescence signal is expected from Nap 2. Furthermore, the charge-neutral HMBQ-Nap 1 should enter cells readily via a passive route, so as to allow for class-selective reporting of biological thiol presence.



**Spectral Properties of Probe/Reporter System.** To demonstrate the off-on nature of the probe 1/reporter 2 system, the fluorescence emission spectra and quantum yields ( $\Phi$ ) of pure HMBQ-Nap 1 probe and pure Nap 2 reporter were obtained in aqueous medium at physiological pH (Figure 1). On the basis of its extremely low-intensity emission spectrum (Figure 1B) and miniscule quantum yield ( $\Phi_{\text{probe}} = 0.003$ ), the fluorescence of HMBQ-Nap 1 probe is quenched in a highly effective manner. We attribute this characteristic to HMBQ-Nap 1 being efficiently PeT-quenched, as a result of its design (electronic properties of the Nap 2 reporter and HMBQ quencher), with the free energy of the PeT quenching process being quite favorable,  $-0.95$  eV (eq 1).<sup>7</sup> On the contrary, free Nap 2 reporter is strongly fluorescent, with a quantum yield ( $\Phi_{\text{reporter}}$ ) of 0.19 in the aqueous medium used here, resulting in a 64-fold difference in quantum efficiency versus the HMBQ-Nap 1 probe.

The absorption maximum of Nap 2 is red-shifted by  $\sim 70$  nm from that of the HMBQ-Nap 1 probe (Figure 1), leading to a  $\sim 4$ -fold higher molar extinction coefficient for Nap 2 at its excitation maximum. This difference in maximum absorption energy is due to the electron-withdrawing capability of the carbamate linkage between the HMBQ and naphthalimide groups in probe 1. Upon excitation at the absorption maximum of Nap 2, the resulting fluorescence emission intensity for Nap 2 at 540 nm is determined to be 64 times greater than that of HMBQ-Nap 1. The  $\sim 275\times$  difference in reporter/probe brightness ( $\epsilon\Phi$ ) observed in Figure 1 makes the reporter/probe pair an excellent candidate for detection and quantification of biological thiols and in high signal-to-background cellular imaging of biological thiols.

**In Vitro Response and Selectivity of Probe to Biological Thiols.** We determined the ability of HMBQ-Nap 1 to act as a turn-on probe when in the presence of only select biological thiols by exposing aqueous, buffered solutions of HMBQ-Nap 1 to three physiologically significant nonprotein thiols: GSH, Cys, and Hcy (Figure 2). Outcomes from both  $^1\text{H}$

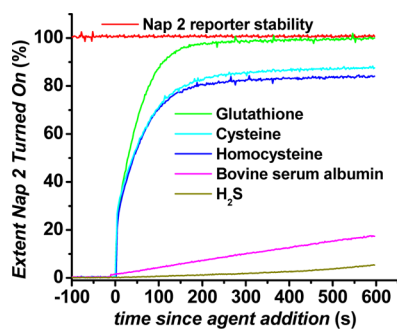


**Figure 2.** Time-dependent fluorescence ( $\lambda_{\text{ex}} = 432$  nm,  $\lambda_{\text{em}} = 540$  nm) from 10  $\mu\text{M}$  HMBQ-Nap 1 incubated with 50  $\mu\text{M}$  thiol-containing analyte in 0.1 M PBS/DMSO (9:1), pH 7.4 at 25  $^{\circ}\text{C}$ . Fluorescence signals were compared to that from a 10  $\mu\text{M}$  solution of Nap 2. Stability of 10  $\mu\text{M}$  Nap 2 with 1 mM GSH is demonstrated by the red line.

NMR and mass spectrometric studies demonstrate that thiols undergo Michael addition to HMBQ-Nap 1 in aqueous media to unleash Nap 2 reporter and quinone methide products (Figures S2 and S3 in Supporting Information); there is no indication of redox activation of HMBQ-Nap 1, as noted by the absence of spectroscopic signatures for reduced HMBQ (hydroquinone). Buffered, aqueous solutions of HMBQ-Nap

1 exhibited an exceedingly rapid increase in fluorescence during their incubation with GSH, Cys, and Hcy, and the rate of fluorescence increase was a function of biological thiol/HMBQ-Nap 1 ratio. Upon evaluation of plots of the fluorescence intensity versus each biological thiol concentration, it was found that there exists an apparent linear relationship for biothiol concentrations up to 2  $\mu\text{M}$  (Figure S4, Supporting Information). From these calibration curves, it was determined that the concentration limits of detection for GSH, Hcy, and Cys are 33, 21, and 29 nM, respectively; the concentration limits of quantification are 110, 70, and 98 nM.<sup>8</sup> The rapid nature of the turn-on process is evidenced by the  $\sim 150$  s time required to reach 90% of the maximum attainable signal for each of the nonprotein thiols GSH, Hcy, and Cys. *This rapid rate of turn-on is unprecedented for a probe system that is able to efficiently generate reporter signal at such low probe/thiol ratios* (substoichiometric, see Figure S4 in Supporting Information; see also Table S1 for comparison to other systems). As expected for this group of biological thiols (similar thiol  $\text{pK}_{\text{a}}$  value)<sup>9</sup> and the HMBQ trigger group,<sup>10</sup> there is no significant difference in fluorescence signal profile. At this time, it is not known why the maximum achievable signal plateau is larger for GSH versus Cys and Hcy.

The potential sulfur-based, cross-reactive species  $\text{H}_2\text{S}$  and bovine serum albumin (BSA) were chosen for initial evaluation of HMBQ-Nap 1 selectivity.  $\text{H}_2\text{S}$ , or more appropriately  $\text{HS}^-$  at physiological pH, has become an increasingly studied species in cells due to its link to cellular signaling pathways and a variety of inflammatory-associated diseases.<sup>11</sup> Although its cellular concentration (nanomolar) is estimated to be dwarfed by that of the more abundant biological thiols,<sup>11</sup>  $\text{H}_2\text{S}$  could possibly be an interferent because of the potential for it to undergo Michael addition to,<sup>12</sup> or cause reduction of, the HMBQ group. In addition, the protein content is roughly 20–25 wt % inside cells, with many of those proteins possessing free thiol groups.<sup>13</sup> Furthermore, over 90% of the extracellular thiols in blood are due to the presence of the most abundant protein ( $\sim 60\%$ ), serum albumin.<sup>14</sup> Human serum albumin (HSA), like BSA, has only one free thiol (Cys 34);<sup>15</sup> this is a potential site of reaction with HMBQ-Nap 1. BSA was chosen for study here due to the known variability in the free thiol content of Cys 34 in HSA upon its storage.<sup>15</sup>

From the kinetic studies in Figure 2, it is found that in stark contrast to the rapid reaction of HMBQ-Nap 1 with GSH, Cys, and Hcy, an exceedingly sluggish response is observed for probe 1 in the presence of  $\text{H}_2\text{S}$  and BSA under equivalent conditions. At 150 s, the signal from GSH is 103-fold higher than that from  $\text{H}_2\text{S}$  and 17 times greater than for BSA. However, we have found that the fluorescence quantum yield of Nap 2 is roughly 25% higher in the presence of 50  $\mu\text{M}$  BSA (conditions in Figure 2), possibly due to viscosity and hydrophobic interaction effects; thus, the selectivity of HMBQ-Nap 1 activation by GSH, Cys, or Hcy versus BSA is certainly higher. The slow reaction of the thiol (Cys 34) in BSA with HMBQ-Nap 1 can be attributed to it being sterically hindered, as the thiol of Cys 34 is oriented toward the interior of the protein,<sup>16</sup> an observation that is consistent with the slow reactivity of Cys 34 in HSA with Ellman's reagent [5,5'-dithiobis(2-nitrobenzoic acid)].<sup>17</sup> We posit that the low reactivity of  $\text{H}_2\text{S}$  with HMBQ-Nap 1 is due to the lack of either HMBQ reduction by  $\text{H}_2\text{S}$  or its Michael addition to HMBQ. The reduction potential of HMBQ in probe 1 is  $-0.80$  V versus SHE in comparison to 0.17 V<sup>18</sup> for  $\text{H}_2\text{S}$ , and successful

Michael addition of  $\text{H}_2\text{S}$  requires a very electron-deficient acceptor.<sup>12,19</sup>

To further delineate the selectivity of HMBQ-Nap 1 activation by GSH, Cys, and Hcy, we examined probe stability under physiological solution conditions in the presence of select amino acids and reducing agents that may activate HMBQ-Nap 1 and yield Nap 2 reporter. Upon inspection of Figure 3, it is clear that the three thiol-free amino acids (1 mM,

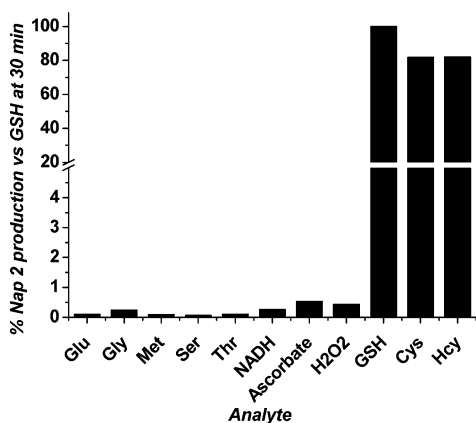


**Figure 3.** Fluorescence response of HMBQ-Nap 1 (10  $\mu\text{M}$ ) incubated at 25  $^{\circ}\text{C}$  for 30 min with 1 mM amino acids and common reductants in 10% DMSO/90% 0.1 M PBS, pH 7.4. Bars represent percent release of free Nap 2 reporter with respect to that achieved for HMBQ-Nap 1 incubated with GSH for 30 min.

100 equiv) with the potential to undergo Michael addition to the HMBQ unit do not interact with HMBQ-Nap 1. Furthermore, the biological reductants NADH ( $E_{1/2} = -0.31\text{ V}$ )<sup>20</sup>—present at millimolar levels within cells—and the ubiquitous ascorbic acid ( $E_{1/2} = 0.051\text{ vs SHE}$ )<sup>21</sup> also did not induce the release of Nap 2 from HMBQ-Nap 1. The lack of redox-induced activation of HMBQ-Nap 1 by these species is in agreement with the observations above with  $\text{H}_2\text{S}$ , as the reduction potentials of these possible interferents are not sufficient to allow reduction of the HMBQ unit in probe 1 ( $-0.80\text{ V vs SHE}$ ).

The temporal integrity of the fluorescence signal generated by production of Nap 2 reporter was investigated so as to test for possible biological thiol-induced structural alterations of the Nap 2 reporter. It was found that the fluorescence intensity of Nap 2 was invariant when the reporter was treated with 100 equiv of GSH (1 mM, Figure 2, red line) for up to 2000 s of incubation, the maximum time tested.

#### Imaging of Biological Thiol Presence in Human Cells.

Upon demonstration that HMBQ-Nap 1 allows for class-selective detection of GSH, Cys, and Hcy under low probe/analyte conditions, an investigation was undertaken to examine the ability of HMBQ-Nap 1 to act as an imaging agent for the presence of these biological thiols in human cells. The ability of HMBQ-Nap to detect thiols in live cells was evaluated using the human lung cancer cell line H596, which is known to have a GSH content of  $140 \pm 70\text{ nmol}\cdot(\text{mg of protein})^{-1}$ .<sup>22</sup> Two-dimensional cell cultures were incubated with 20  $\mu\text{M}$  HMBQ-Nap 1 for 10 min at 37  $^{\circ}\text{C}$  and subsequently washed with 0.1 M PBS, pH 7.4, and then the cells were fixed with formaldehyde. As the negative-control/background experiment, H596 cells were preincubated with 10 mM *N*-ethylmaleimide (NEM) at 37  $^{\circ}\text{C}$  for 30 min to scavenge thiols in the cells, and then the

cells were washed with 0.1 M PBS, pH 7.4, to remove excess NEM, followed by incubation with 20  $\mu\text{M}$  HMBQ-Nap 1 for 10 min prior to their being fixed as above. Fluorescence images were obtained by confocal laser microscopy via excitation at 458 nm and detection at 458–514/514–680 nm, with integrated cellular fluorescence intensity being obtained via software.

Unadulterated H596 cells that were exposed to HMBQ-Nap 1 exhibited strong fluorescence (Figure 4, without NEM),

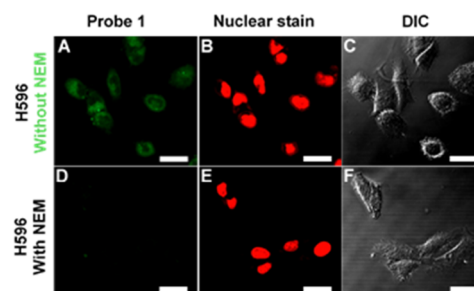


**Figure 4.** Microscopic images of human H596 lung cells, (A–C) incubated for 10 min at 37  $^{\circ}\text{C}$  with 20  $\mu\text{M}$  HMBQ-Nap 1 and (D–F) preincubated with 10 mM NEM thiol scavenger for 30 min at 37  $^{\circ}\text{C}$ , followed by incubation with HMBQ-Nap 1 for 10 min at 37  $^{\circ}\text{C}$ . (A, B, D, E) Confocal laser microscopy; (C, F) differential interference contrast (DIC). Scale bar = 20  $\mu\text{m}$ .

whereas there was no apparent fluorescence in the negative control cells that were pretreated with thiol scavenger (Figure 4, with NEM). A signal-to-background ratio of 4.2 was obtained upon comparison of the integrated fluorescence intensities for the untreated and NEM-treated cells (13 and 17 sample replicates, respectively); to the best of our knowledge, the work here is the first report of this analytical figure of merit for biological thiol imaging in cells. Thus, electrically neutral HMBQ-Nap 1 is able to enter cells and report on the presence of intracellular biological thiols in a rapid and selective fashion (10 min).

## CONCLUSIONS

We have designed, synthesized, and made viable a new dual quenching/trigger group-based probe whose PeT-quenched fluorescence signal is turned on selectively upon rapid reaction of probe trigger group with biologically important thiols so as to cause probe shedding of the thiol-activated trigger group. The probe HMBQ-Nap 1 exhibits high selectivity and rapid response toward the three biological thiols glutathione, cysteine, and homocysteine, when compared to protein-associated thiol or the simple gasotransmitter  $\text{H}_2\text{S}$ , as well as other potential interferents commonly found in mammalian systems. Rapid activation of HMBQ-Nap 1 by thiols to yield the highly fluorescent reporter Nap 2 is attributed to thiol-addition-initiated elimination of the trigger group. Furthermore, it has been successfully demonstrated that HMBQ-Nap 1 can provide such rapid and selective thiol detection in human cells, and with an exceedingly low limit of detection under in vitro conditions where there is no need for excessive amounts of probe 1, unlike previously reported probes that require probe/thiol ratios of 70:1 to 5000:1.<sup>3a</sup> Thus, HMBQ-Nap 1 diversifies the pool of biological thiol probes by offering rapid, class-selective detection and quantification with high figures of merit.

## ■ ASSOCIATED CONTENT

### ■ Supporting Information

Additional text describing materials and general methods, synthesis of 2, 3, and 5–8, NMR kinetic experiments, MS experiments, and characterization data; one scheme showing synthesis of HMBQ-Nap 1; four figures illustrating design concept of fluorescent probe HMBQ-Nap 1, NMR spectra, negative-ion mass spectra, and fluorescence spectral changes; and one table listing comparison of HMBQ-Nap 1 properties to those of other GSH, Cys, and Hcy class-responsive probes. This material is available free of charge via the Internet at <http://pubs.acs.org>.

## ■ AUTHOR INFORMATION

### Corresponding Author

\* E-mail [tunnel@LSU.edu](mailto:tunnel@LSU.edu); fax 225-578-3458; tel 225-578-3458.

### Author Contributions

All authors have given approval to the final version of the manuscript.

### Notes

The authors declare no competing financial interest.

## ■ ACKNOWLEDGMENTS

This material is based upon work supported by the U.S. National Institutes of Health (SR21CA135585, P42ES013648) and the U.S. National Science Foundation under Grant CHE-0910845. R.R.N. and S.U.H. are grateful for LSU Graduate School Fellowships. B.P. thanks the Louisiana Economic Development Assistantship Program at LSU.

## ■ REFERENCES

- (1) Kobayashi, H.; Choyke, P. L. *Acc. Chem. Res.* **2011**, *44*, 83–90.
- (2) Sun, Y.-Q.; Chen, M.; Liu, J.; Lv, X.; Li, J.-f.; Guo, W. *Chem. Commun.* **2011**, 47, 11029–11031.
- (3) (a) See Table S-1 in Supporting Information. (b) Lee, M. H.; Han, J. H.; Kwon, P.-S.; Bhuniya, S.; Kim, J. Y.; Sessler, J. L.; Kang, C.; Kim, J. S. *J. Am. Chem. Soc.* **2011**, *134*, 1316–1322. (c) Li, Y.; Yang, Y.; Guan, X. *Anal. Chem.* **2012**, *84*, 6877–6883. (d) Long, L.; Zhou, L.; Wang, L.; Meng, S.; Gong, A.; Du, F.; Zhang, C. *Org. Biomol. Chem.* **2013**, *11*, 8214–8220. (e) Kim, G.-J.; Lee, K.; Kwon, H.; Kim, H.-J. *Org. Lett.* **2011**, *13*, 2799–2801. (f) Lim, C. S.; Masanta, G.; Kim, H. J.; Han, J. H.; Kim, H. M.; Cho, B. R. *J. Am. Chem. Soc.* **2011**, *133*, 11132–11135. (g) Guo, X.-F.; Chen, J.-B.; Wang, H.; Zhang, H.-S.; Huang, W.-H.; Guo, J. *Talanta* **2012**, *99*, 1046–1050.
- (4) Montoya, L. A.; Pluth, M. D. *Anal. Chem.* **2014**, *86*, 6032–6039.
- (5) Giraud, L.; Giraud, A. *Synthesis* **1998**, 1153–1160.
- (6) Fery-Forgues, S.; Lavabre, D. *J. Chem. Educ.* **1999**, *76*, 1260.
- (7) Silvers, W. C.; Prasai, B.; Burk, D. H.; Brown, M. L.; McCarley, R. L. *J. Am. Chem. Soc.* **2013**, *135*, 309–314.
- (8) The concentration limit of detection is defined as the concentration that corresponds to  $3s_{\text{blank}}/\text{slope}$  of the calibration curve. The concentration limit of quantification is defined as the concentration that corresponds to  $10s_{\text{blank}}/\text{slope}$  of the calibration curve.
- (9) Lash, L. H.; Jones, D. P. *Arch. Biochem. Biophys.* **1985**, *240*, 583–592.
- (10) Huang, S.-T.; Ting, K.-N.; Wang, K.-L. *Anal. Chim. Acta* **2008**, *620*, 120–126.
- (11) Li, L.; Rose, P.; Moore, P. K. *Annu. Rev. Pharmacol. Toxicol.* **2011**, *51*, 169–187.
- (12) Perlinger, J. A.; Kalluri, V. M.; Venkatapathy, R.; Angst, W. *Environ. Sci. Technol.* **2002**, *36*, 2663–2669.
- (13) Ellis, R. J. *Trends Biochem. Sci.* **2001**, *26*, 597–604.
- (14) Nicholson, J. P.; Wolmarans, M. R.; Park, G. R. *Br. J. Anaesth.* **2000**, *85*, 599–610.
- (15) Tong, G. Characterization of Cysteine-34 in Serum Albumin. Ph.D. thesis, The Ohio State University, Columbus, Ohio, 2003.
- (16) Turell, L.; Radi, R.; Alvarez, B. *Free Radical Biol. Med.* **2013**, *65*, 244–253.
- (17) Torres, M. J.; Turell, L.; Botti, H.; Antmann, L.; Carballal, S.; Ferrer-Sueta, G.; Radi, R.; Alvarez, B. *Arch. Biochem. Biophys.* **2012**, *521*, 102–110.
- (18) Collman, J. P.; Ghosh, S.; Dey, A.; Decréau, R. A. *Proc. Natl. Acad. Sci. U.S.A.* **2009**, *106*, 22090–22095.
- (19) Liu, C.; Peng, B.; Li, S.; Park, C.-M.; Whorton, A. R.; Xian, M. *Org. Lett.* **2012**, *14*, 2184–2187.
- (20) Carlson, B. W.; Miller, L. L. *J. Am. Chem. Soc.* **1985**, *107*, 479–485.
- (21) Ball, E. G. *J. Biol. Chem.* **1937**, *118*, 219–239.
- (22) Carmichael, J.; Mitchell, J. B.; Friedman, N.; Gazdar, A. F.; Russo, A. *Br. J. Cancer* **1988**, *58*, 437–440.